

# Optimized *Eleutherine bulbosa* Urb. bulb extract on the inhibition of 3D retinoblastoma spheroids cultured in type I murine collagen

Ammar Akram Kamarudin<sup>1,2</sup>, Nor Hafiza Sayuti<sup>2</sup>, Mohamad Zulhafiz Shafiq Zulhilmi Cheng<sup>2,3</sup>, Norazalina Saad<sup>4</sup>, Nur Hanisah Azmi<sup>5</sup>, Norhaizan Mohd. Esa<sup>2,6</sup>

<sup>1</sup>School of Biology, Faculty of Applied Sciences, Universiti Teknologi MARA (UiTM), Cawangan Negeri Sembilan, Kampus Kuala Pilah, Kuala Pilah 72000, Negeri Sembilan, Malaysia

<sup>2</sup>Natural Medicines and Product Research Laboratory (NaturMeds), Institute of Bioscience, Universiti Putra Malaysia, Serdang 43400, Selangor, Malaysia

<sup>3</sup>Department of Technology and Natural Resources, Faculty of Applied Sciences and Technology, Universiti Tun Hussein Onn Malaysia (UTHM), Hab Pendidikan Tinggi Pagoh, Pagoh 84600, Johor, Malaysia

<sup>4</sup>Laboratory of Cancer Research UPM-MAKNA (CANRES), Institute of Bioscience, Universiti Putra Malaysia, Serdang 43400, Selangor, Malaysia

<sup>5</sup>Nutrition in Community Engagement (NICE) Living Laboratory, Faculty of Food Science and Nutrition, Universiti Malaysia Sabah, Jalan UMS, Kota Kinabalu 88400, Sabah, Malaysia

<sup>6</sup>Department of Nutrition, Faculty of Medicine and Health Sciences, Universiti Putra Malaysia, Serdang 43400, Selangor, Malaysia

**Correspondence to:** Norhaizan Mohd. Esa. Department of Nutrition, Faculty of Medicine and Health Sciences, Universiti Putra Malaysia, Serdang 43400, Selangor, Malaysia. nhaizan@upm.edu.my

Received: 2024-10-31 Accepted: 2024-12-18

## Abstract

• **AIM:** To investigate the efficacy of *Eleutherine bulbosa* (Mill.) Urb. bulb extract (EBE) on the 3D human retinoblastoma cancer cells (WERI-Rb-1) spheroids and explore its apoptotic mechanism.

• **METHODS:** The 3D WERI-Rb-1 and human retinal pigmented epithelium cells (ARPE-19) spheroids were developed using type 1 murine collagen that was excised from the rat tail tendon and cultured *via* hanging drop and embedded techniques. The cytotoxic activity was examined by Alamar blue assay meanwhile, the morphological

characteristics were assessed by 4',6-diamidino-2-phenylindole (DAPI) and scanning electron microscopy (SEM). The mRNA and protein expressions of apoptotic and antioxidant signal transduction pathways were explored to ascertain its molecular mechanisms. The statistical analysis was carried out using GraphPad Prism.

• **RESULTS:** The Alamar blue assay portrayed higher half maximal inhibitory concentration (IC<sub>50</sub>) values of EBE and cisplatin on 3D WERI-Rb-1 model as compared to the previous study on 2D model. The results of DAPI and SEM illustrated apoptotic features upon treatment with EBE and cisplatin in a dose-dependent manner on 3D WERI-Rb-1 model. The mRNA and protein levels of apoptotic and antioxidant-related pathways were significantly affected by EBE and cisplatin, respectively ( $P < 0.05$ ). The regulation of gene and protein expressions of 3D WERI-Rb-1 spheroids differed from the 2D study, suggesting that the tumor microenvironment of extracellular matrix (ECM) collagen matrix hindered the EBE treatment efficacy, leading to apoptotic evasion.

• **CONCLUSION:** A significant inhibition effect of EBE is observed on the 3D WERI-Rb-1 spheroids. The presence of ECM causes an increase in cytotoxic resistance upon treatment with EBE and cisplatin.

• **KEYWORDS:** *Eleutherine bulbosa* Urb; 3D WERI-Rb-1 spheroids; apoptotic; antioxidants

**DOI:10.18240/ijo.2025.05.05**

**Citation:** Kamarudin AA, Sayuti NH, Cheng ZHZ, Saad N, Azmi NH, Mohd Esa N. Optimized *Eleutherine bulbosa* Urb. bulb extract on the inhibition of 3D retinoblastoma spheroids cultured in type I murine collagen. *Int J Ophthalmol* 2025;18(5):802-812

## INTRODUCTION

Retinoblastoma (Rb) is a genetically rare ocular cancer that is prevalent among children. Current management of Rb involves eye salvation, visual function, and patient care<sup>[1]</sup>. Chemotherapy and radiotherapy are commonly used to

treat Rb, however, these treatments gradually damage healthy cells and cause treatment resistance<sup>[2]</sup>. Therefore, the urge for alternative and complementary options with minimum side effects are warranted. Locally known as a Dayak onion, the bulb of *E. bulbosa* is indigenous among the aboriginal Dayak people with a long history of treating diabetes, breast cancer, hypertension, stroke, sexual disorder, and breast milk production<sup>[3]</sup>. Our review unraveled its pharmacological activities *i.e.* cytotoxic, anti-diabetic, anti-microbial, anti-inflammatory, antioxidant, dermatological and reproductive problems, as well as its potential applications<sup>[4]</sup>. Under optimized extraction condition, the bulb exerted a potent cytotoxic potential against Rb cells induced by the synergistic effect of the bioactive compounds *i.e.* eleutherin, gallic acid, chlorogenic acid, quercetin, kaempferol, rutin, epicatechin gallate and myricetin<sup>[5-6]</sup>. The traditional monolayer two-dimensional (2D) cell culture has been widely utilized for its simplicity and low economic cost but have major drawbacks *i.e.* forced polarity, biochemical signals, and cell-to-cell communication, rendering unrealistic tissue physiological environment<sup>[7]</sup>. In view of this, alternative approach should be focused to captivate successful drug response mechanisms. The advance of state-of-the-art cancer biomarkers and preclinical models with enhanced drug bioavailability is promising routes to recapitulate *in vivo* tumor biology and microenvironment<sup>[8]</sup>. Three-dimensional (3D) cell culture offers fascinating features in myriad applications of tissue engineering *i.e.* response to stimuli, differentiation, drug metabolism, cell morphology and proliferation<sup>[9]</sup>. Collagen and Matrigel are frequently used in developing 3D cell culture models for their remarkable biocompatibility and natural adhesive properties that support various physiological cell functions, resulting in enhanced cell viability, controlled proliferation, and differentiation<sup>[8]</sup>. Extracellular matrix (ECM) consisting of matrix proteins, glycoproteins, glycosaminoglycans, and proteoglycans facilitate successful regulation of cell proliferation, migration, differentiation, adhesion and survivability<sup>[10]</sup>. The structure of ECM influences drug response to cells by regulating drug mechanism of action and drug resistance<sup>[10]</sup>. Scaffold-based and scaffold-free techniques are the most favorable approaches in ECM applications for the development of a successful 3D cell culture model. Scaffold-based like hydrogels are distinctive as they permit soluble factors *i.e.* cytokines and growth factors through a network of tissue-like gels<sup>[8]</sup>. Natural hydrogels for instance collagen and Matrigel are quintessential ECM applications for their remarkable biocompatibility and natural adhesive properties that support various physiological cell functions, resulting in enhanced cell viability, controlled proliferation, and differentiation, typically observed in an *in vivo* environment<sup>[8]</sup>. They stimulate cell adherent *via* integrin

receptors that activates cell signaling pathway, which is essential for cell survivability, growth, and proliferation<sup>[11-12]</sup>. Nevertheless, batch-to-batch variability in Matrigel limits its application in tissue engineering as it causes interference with the pharmacological activity of the drug response<sup>[8]</sup>. Unlike collagen, batch variability could be minimized and more convenient to alter the concentrations, allowing changes in hydrogel stiffness as well as cell proliferation<sup>[12-13]</sup>. Therefore, this study highlighted the development of a novel 3D retinoblastoma spheroids, derived from the human retinoblastoma cancer cells (WERI-Rb-1) cell line using collagen type I as ECM matrix. Then, the efficacy of the optimized *Eleutherine bulbosa* (Mill.) Urb. bulb extract (EBE) would be observed towards the inhibition of the 3D retinoblastoma spheroids through the regulation of gene and protein expressions.

## MATERIALS AND METHODS

**Ethical Approval** This study was approved by the Institutional Animal Care and Use Committee, Universiti Putra Malaysia (Ethics Code: UPM/IACUC/2019/R008).

**Cell Lines and Reagents** WERI-Rb-1 (ATCC<sup>®</sup> HTB-169<sup>™</sup>) and human retinal pigmented epithelium cells (ARPE-19, ATCC<sup>®</sup> CRL-2302<sup>™</sup>) were acquired from the American Type Culture Collection (Manassas, VA, USA). Roswell Park Memorial Institute 1640 (RPMI-1640) and Dulbecco's Modified Eagle (DMEM/F12) medium was purchased from Nacalai Tesque, Inc, Japan. Fetal bovine serum (FBS) was obtained from Life Technologies/Gibco Co. (Carlsbad, CA, USA). Resazurin sodium salt, phosphate buffer saline (PBS), cisplatin, 4',6-diamidino-2-phenylindole (DAPI), and propidium iodide was purchased from Sigma-Aldrich (St. Louis, MO, USA). Ethanol, acetic acid, and chloroform was obtained from Merck KGaA (Germany).

**Plant Materials and Extraction** The bulb of *E. bulbosa* was purchased from the Probolinggo, East Java, Indonesia. Identification of plant sample was conducted by Biodiversity Unit, Institute of Bioscience, UPM Serdang, Selangor, Malaysia (Voucher specimen: MFI 0055/19). The bulbs were washed and dry heated in a warm air oven at 40°C overnight. Then, the dried bulbs were grounded to fine powder using a commercial blender, sieved with 400 µm and stored at 4°C for further analysis. The extraction of *E. bulbosa* bulb was conducted according to our previous optimized extraction condition<sup>[6]</sup>. Briefly, 10.0 g of powdered *E. bulbosa* bulb was weighed and mixed with 146 mL of 90% ethanol. The mixture was boiled at 45°C for 70min, filtered with Whatman No.1 filter paper and evaporated through rotary evaporator.

**Cell Culture** WERI-Rb-1 (ATCC<sup>®</sup> HTB-169<sup>™</sup>) and ARPE-19 (ATCC<sup>®</sup> CRL-2302<sup>™</sup>) were acquired from the American Type Culture Collection (Manassas, VA, USA).

The WERI-Rb-1 cells were cultured and maintained in RPMI meanwhile, ARPE-19 cells in DMEM/F12. Both cultures were supplemented with 10% FBS and incubated at 37°C under 5% CO<sub>2</sub>.

**Type I Murine Collagen Preparation** The rat tails were obtained from the Comparative Medicine and Technology Unit (COMeT), Institute of Bioscience, Universiti Putra Malaysia. The collagen isolation was excised according to Rajan *et al*<sup>[14]</sup>. Type I collagen was excised from the rat tail tendon through acid-digestion, lyophilized, and reconstituted in 0.02 mol/L acetic acid at 10 mg/mL. The dissolved collagen was centrifuged at 30 000×g, 4°C for 45min to collect the supernatant. The collagen was sterilized in a dialysis bag containing 0.02 mol/L acetic acid for 1wk, with medium change for every 2 to 3d. After a week, the sterilized stock collagen was collected and stored at 4°C until further used. For 3D WERI-Rb-1 spheroids development, the stock collagen was diluted to 1 mg/mL with complete growth media, and neutralized (pH 6.5-7) with a sterile 0.1 mol/L sodium hydroxide solution (25 µL).

**3D WERI-Rb-1 and ARPE-19 Spheroids** The 3D WERI-Rb-1 and ARPE-19 spheroids were developed *via* hanging drop and embedded culture technique according to Saengwimol *et al*<sup>[11]</sup> with major modifications. At a density of 5×10<sup>4</sup> cells/droplet and 2×10<sup>4</sup> cells/droplet, 20 µL of WERI-Rb-1 and ARPE-19 cells were hung on the lid of the sterile petri dish with complete growth media for 48h under 5% CO<sub>2</sub> at 37°C, respectively. After 48h, each droplet of the hanging drop culture was carefully embedded into microplates containing 10% collagen (1 mg/mL) mixed with a complete growth medium and grew for another 48h under 5% CO<sub>2</sub> at 37°C prior to all experimental assays.

**Cytotoxic Assay** The cytotoxic assay was carried out using Resazurin sodium salt with few adjustments<sup>[15]</sup>. The 3D WERI-Rb-1 and ARPE-19 models were developed as in earlier section with a density of 5×10<sup>4</sup> cells/well and 2×10<sup>4</sup> cells/well in a 96-well plate, respectively. The spheroids were treated with EBE (1000, 500, 250, 100, 50, 25, 10 µg/mL) and cisplatin (C) for 72h. At the end of the treatment period, 100 µL of media was removed. The Alamar blue solution (10 µL of 5 mg/mL) was added into each well and incubated for 24h with under 5% CO<sub>2</sub> at 37°C. The fluorescent intensity was recorded at 560 nm excitation and 590 emissions with a microplate reader (Synergy™ HI Multi-Mode, BioTek, USA). All measurements were conducted in triplicates and calculated as: Percentage difference between treated and control cells: “FI of treated cells”/“FI of untreated cells”×100 where, FI is fluorescence intensity at 590 nm emission and 560 nm excitation.

**Cell Treatments** The inhibitory concentrations (IC) denoted as EBE<sub>25</sub>, EBE<sub>50</sub>, EBE<sub>75</sub>, C<sub>25</sub>, C<sub>50</sub>, and C<sub>75</sub> were extrapolated

from the cytotoxic assay to observe the dose-dependent effects on the developed 3D spheroids models after 72h.

### Morphological Assessments of 3D Retinoblastoma Spheroids

**DAPI and PI dual staining** The DAPI and PI dual staining was carried out with minor adjustments<sup>[16]</sup>. The WERI-Rb-1 spheroids were cultured at a density of 5×10<sup>4</sup> cells/well (10 droplets) in a 24-well plate and treated as described in earlier section. Then, 200 µL of culture medium was removed and incubated with 200 µL of DAPI solution (5 µg/mL) for 15min at 37°C. The spheroids were subsequently treated with 200 µL of PI solution (10 µg/mL) for another 15min at 37°C. Images were captured using a fluorescence microscope (Axio Vert. A1 Carl Zeiss, Göttingen, Germany).

**Scanning electron microscopy** The WERI-Rb-1 spheroids were cultured at a density of 1×10<sup>6</sup> cells/well (20 droplets) in a 6-well plate and treated as described above. The in-house microscopy guideline was conducted accordingly at Microscopy Unit, Institute of Bioscience, UPM. In brief, the 3D WERI-Rb-1 spheroids were fixed with 4% glutaraldehyde and 1% osmium tetroxide for 6 and 2h at 4°C, respectively. The spheroids were washed thrice for 10min at 3000×g with 0.1 mol/L sodium cacodylate buffer to remove the fixative agents. The cell pellets were dehydrated with 35%, 50%, 75%, and 95% acetone for 10min, accordingly. Further dehydration was subjected thrice with 100% acetone for 15min. The spheroids were dried on a critical dryer for 30min and observed under JSM 6400 scanning electron microscope (Joel, USA).

**Gene expression analysis** The spheroids were cultured at a density of 1×10<sup>6</sup> cells/well (20 droplets) in a 6-well plate and treated as described in earlier section. The total RNA was isolated using phenol-chloroform RNA extraction<sup>[17]</sup>. The purity of the RNA was determined using NanoDrop (NanoPhotometer™ Pearl, Munich, Germany). The first strand of cDNA synthesis was performed using iScript™ cDNA Synthesis kit (Bio-Rad, USA). The product of cDNA synthesis was quantitatively determined using iQ™ SYBR® Green Supermix (Bio-Rad, USA) according to the manufacturing protocols. The PCR cycling program was carried out on Bio-Rad CFX-96™ Real-Time System (Bio-Rad, USA) according to the manufacturer’s protocol: 1 cycle of polymerase activation and DNA denaturation at 95°C for 3min, followed by 39 cycles of denaturation at 95°C for 10s, combined annealing, and extension step at 55°C for 30s, respectively. The melting curve analysis was programmed at 65°C to 95°C with an increment of 0.5°C for 5s. The list of primers was outlined as in Table 1. The relative mRNA expression was calculated using the Livak method (2<sup>-ΔΔCT</sup>) in triplicates with glyceraldehyde-3-phosphate dehydrogenase (GAPDH) served as an internal control.

**Table 1** List of the nucleotide sequences used in qPCR

Genes	Accession numbers	Forward primers (3'-5')	Reverse primers (5'-3')
Bcl-xL	NM_001317919.2	ACTCTCCGGGATGGGGTAA	AGGTAAGTGGCCATCCAAGC
Bax	NM_001291428.2	TCATGGGCTGGACATTGGAC	GAGACAGGGACATCAGTCGC
Caspase 3	NM_004346.3	AGGTGACACTATAGAATATCC ATTAAAAATTTGGAACC	GTACGACTCACTATAGGACT TTAGAAACATCACGCATC
Caspase 9	NM_001229.4	AGGTGACACTATAGAATATGT TCAGGCCCCATA	GTACGACTCACTATAGGGACT CAAGAGCACCGACA
NRF-2	NM_006164.4	AGGTGACACTATAGAATATCG CAACAACCTTTATCT	GTACGACTCACTATAGGGAA GAGGAGGTCTCCGTTA
HO-1	NM_002133.2	AGGTGACACTATAGAATAACT GCGTTCCTGCTCAACAT	GTACGACTCACTATAGGGAG GGCAGAATCTTGCACTTTGT
SOD-1	NM_000454.4	AGGTGACACTATAGAATAAA GTACAAAGACAGGAAACG	GTACGACTCACTATAGGGATG ACAAGTTAATACCCATCT
GAPDH <sup>a</sup>	NM_001357943.2	GTCATCCCTGAGCTGAACGG	CCACCTGGTGCTCAGTGTAG

qPCR: Quantitative real time polymerase chain reaction; Bcl-xL: B-cell lymphoma-extra large; Bax: BCL-2 associated X; Caspase: Cysteine-aspartic acid protease; NRF-2: Nuclear factor erythroid 2-related factor; HO-1: Heme oxygenase 1; SOD-1: Superoxide dismutase 1; GAPDH: Glyceraldehyde-3-phosphate dehydrogenase. Based on the *Homo sapiens* gene sequences adopted from the National Centre for Biotechnology Information GenBank Database (NCBI). <sup>a</sup>Housekeeping gene.

**Protein expression analysis** The WERI-Rb-1 spheroids were cultured at a density of  $1 \times 10^6$  cells/well (20 droplets) in a 6-well plate and treated as in earlier section. The total proteins were harvested with RIPA lysis buffer (Nacalai Tesque, Japan). The protein lysate was quantified using Pierce™ BCA Protein Assay kit (Thermo Fisher, USA). The total protein was subjected to electrophoresis on 10% sodium dodecyl sulfate-polyacrylamide gel electrophoresis (SDS-PAGE) for 90min at 120 V, followed by a semi-dry transfer onto polyvinylidene fluoride (PVDF) membranes (Bio-Rad, USA) for 45min. The membrane was blocked with 3% skimmed milk for 1h prior to the incubation of primary antibodies *i.e.* GAPDH mouse (1:1000, ABclonal, USA), GAPDH rabbit (1:1000, ABclonal, USA), nuclear factor erythroid 2-related factor (NRF-2; 1:1000, ABclonal, USA), heme oxygenase 1 (HO-1; 1:500, ABclonal, USA), superoxide dismutase 1 (SOD-1; 1:1000, Cell Signaling Technology®), Caspase 3 (1:500, ABclonal, USA), Caspase 8 (1:1000, ABclonal, USA), Caspase 9 (1:1000, ABclonal, USA), B-cell lymphoma-extra large (Bcl-xL; 1:1000, ABclonal, USA), BCL-2 associated X (Bax; 1:1000, ABclonal, USA) and incubated for overnight at 4°C. Following thrice TBST wash for 10 min the next day, the membrane was incubated with secondary antibodies *i.e.* horseradish peroxidase-conjugated anti-mouse and anti-rabbit antibodies (1:10000, ABclonal, USA) for 1h. Immunoreactive bands were determined using WesternBright® ECL HRP substrate (Advansta, San Jose, USA) in 1:1 ratio for 2min and the images were captured *via* FluorChem™ E System (ProteinSimple, USA). The relative densities of the blots were analyzed using Image J software.

**Statistical Analysis** The statistical analysis was carried out using GraphPad Prism (USA). Data were expressed as

**Table 2** The cytotoxic concentrations of the respective tested compounds

Test compounds	IC <sub>25</sub>	IC <sub>50</sub>	IC <sub>75</sub>
EBE	25.5±0.9	45.7±1.7	128.4±5.7
Cisplatin	11.9±2.2	26.6±6.0	44.3±5.2

All measurements were conducted in triplicates and expressed as mean±standard deviations. IC: Maximal inhibitory concentration; EBE: *Eleutherine bulbosa* (Mill.) Urb. bulb extract.

mean±standard deviation. The inhibitory concentrations were established by non-linear regression analysis. The statistical difference was analyzed by one-way analysis of variance (ANOVA) followed by Tukey post hoc test.  $P < 0.05$  was considered as statistically significant.

## RESULTS

**Cytotoxic Assay** Table 2 demonstrated the effect of both treatments towards the inhibition of 3D WERI-Rb-1 spheroids. The results of EBE<sub>50</sub> was 45.7±1.7 µg/mL meanwhile, cisplatin recorded a C<sub>50</sub> value of 26.6±6.0 µg/mL, respectively. It was observed that the EBE<sub>50</sub> was 2.9-fold higher than our previous study on 2D WERI-Rb-1 cells<sup>[5]</sup>. The C<sub>50</sub> value also presented a remarkable increase in 3D model with 7.4-fold higher than the 2D model (3.6 µg/mL). The results highlighted that the 3D WERI-Rb-1 spheroids manifested higher resistance of drug sensitivity upon treatment with EBE and cisplatin compared to our previous study on 2D model<sup>[5]</sup>. On the other hand, the 3D ARPE-19 spheroids demonstrated higher IC<sub>50</sub> value (>200 µg/mL, data not shown), indicating that the EBE was not toxic to normal cells. It was also noted that the IC<sub>50</sub> value of the 3D ARPE-19 spheroids increases in comparison to our previous study<sup>[5]</sup>.

## Surface Morphology of 3D WERI-Rb-1 Spheroids

**DAPI and PI dual staining** To further observe the cytotoxic

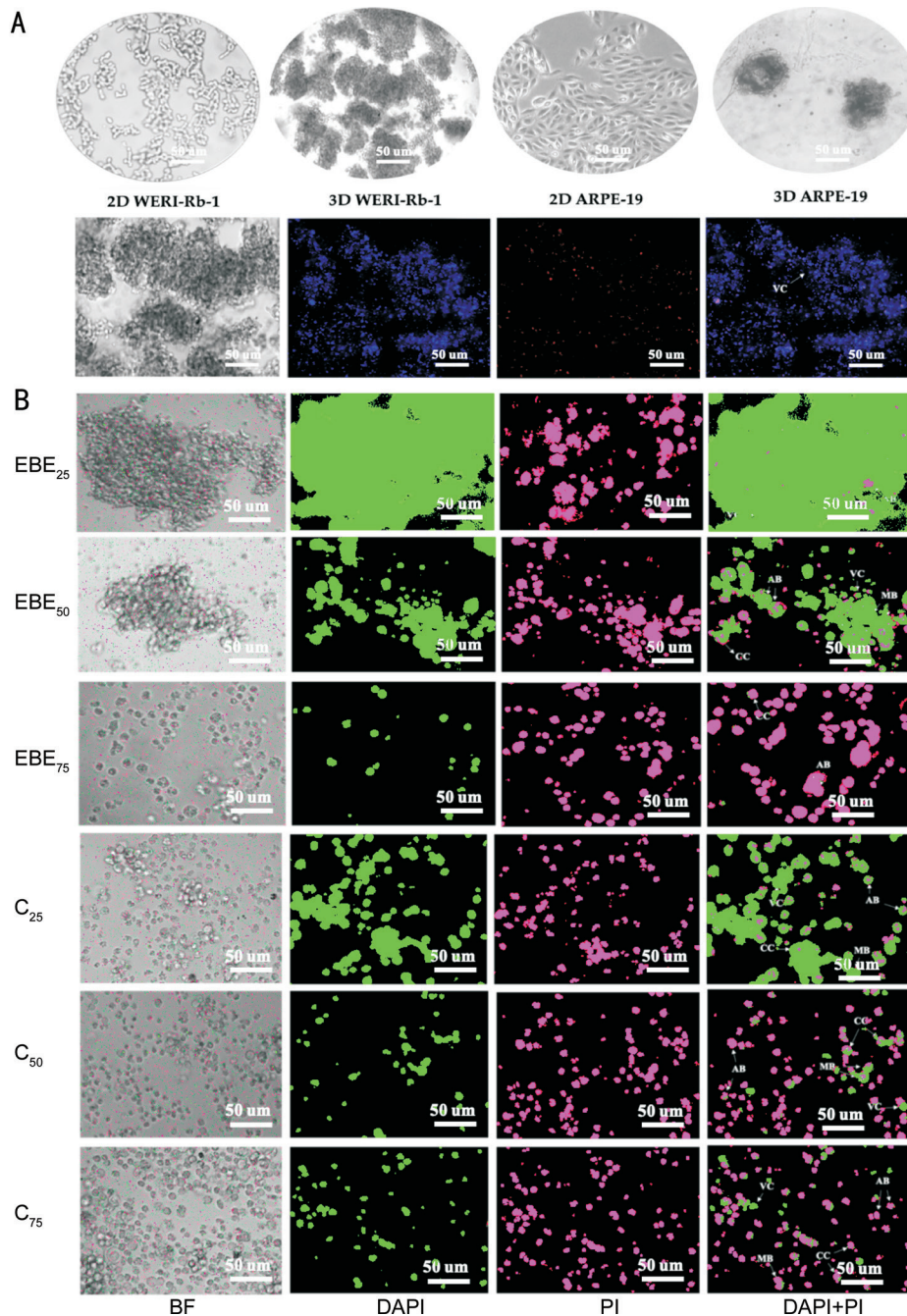


**Figure 1** Comparison between 2D, 3D WERI-Rb-1 and ARPE-19 cultures (A) and the morphological evaluation of WERI-Rb-1 spheroids upon treatments as compared to the untreated (B) AB: Apoptotic bodies; BF: Brightfield; CC: Chromatin condensation; MB: Membrane blebbing; VC: Viable cells. Magnification: 400×, Scale bar: 50 μm.

effect of both treatments on the developed 3D WERI-Rb-1 model, morphological evaluation was conducted *via* DAPI and PI double staining. Figure 1A portrayed the structural differences of the untreated group between 2D and 3D WERI-Rb-1 and ARPE-19 spheroids, respectively.

Figure 1B demonstrated apoptotic features in a dose-dependent manner upon treatment with EBE and cisplatin, respectively. Under brightfield exposure, the disruption of 3D WERI-Rb-1 spheroids were remarkably noticed with increase concentrations of both treatments.

**Scanning electron microscopy** Figure 2 depicts the formation

of cellular aggregates in a 3D environment. Meanwhile, a stretchable grape-like cluster morphology was observed in the 2D culture, as captured in Figure 1. The collagen fibers acting as an ECM matrix orchestrate the cytoskeletal organization of 3D spheroids by facilitating cellular signalling, cell movement, and nutrient diffusion. Besides that, cellular disruption and apoptotic bodies became more apparent with increasing concentrations of EBE and cisplatin, respectively. The apoptotic effect of EBE could be associated with the synergistic interaction of the bioactive compounds reported in the previous study<sup>[6]</sup>.

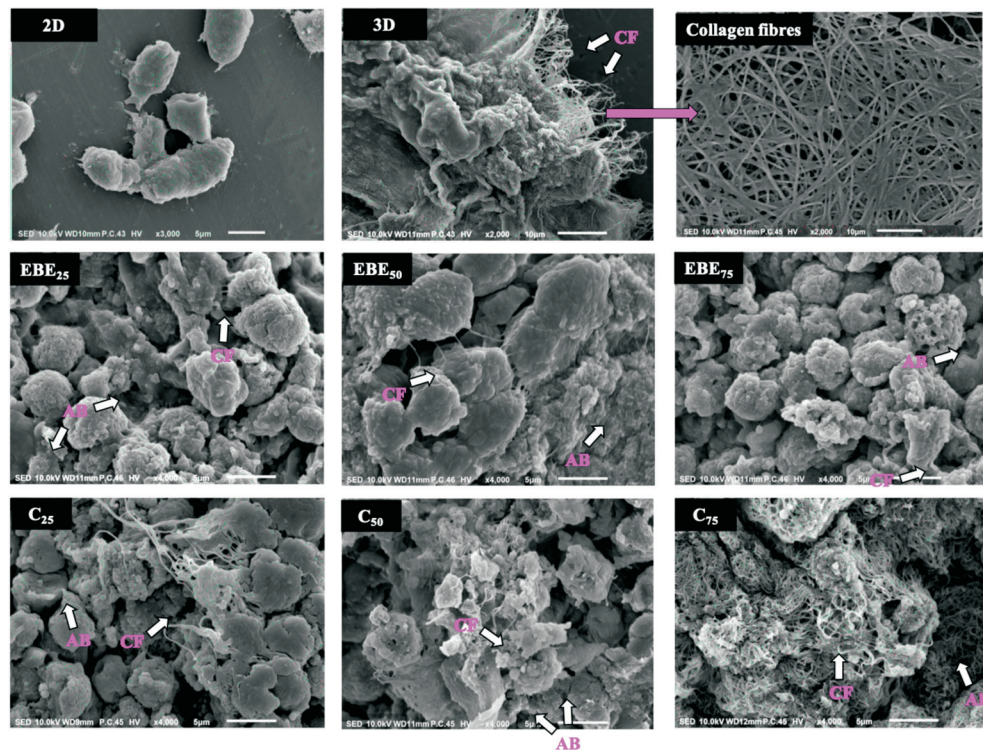


**Figure 2** The surface morphological observation between 2D and 3D untreated WERI-Rb-1 models, respectively Cell disruption was noticeable in 3D WERI-Rb-1 spheroids as concentrations of EBE and cisplatin increases. Remarks; CF: Collagen fibres; AB: Apoptotic bodies; EBE: Eleutherine bulbosa (Mill.) Urb. bulb extract.

**Modulatory Effect of EBE on mRNA and Protein Expressions of WERI-Rb-1 Spheroids** Figure 3A displayed the mRNA expression of *Bax* gene that was significantly upregulated ( $P < 0.05$ ) in a dose-dependent manner upon both treatments as compared to the untreated group, except  $EBE_{25}$  ( $P > 0.05$ ). Interaction between treatments revealed a significant different between  $EBE_{25}$  versus  $EBE_{50}$  and  $EBE_{75}$  ( $P < 0.05$ ). No effect observed between  $EBE_{50}$  and  $EBE_{75}$  treatments ( $P > 0.05$ ). For cisplatin, treatment difference was only observed between  $C_{25}$  and  $C_{75}$  ( $P < 0.05$ ). Figure 3B displayed a significant upregulation of Bax protein ( $P < 0.05$ ) compared to the untreated group. Treatment with  $C_{75}$  displayed no significant different in contrast to the untreated group ( $P > 0.05$ ) meanwhile,  $EBE_{75}$  recorded the highest Bax expression in comparison to other treatments, significantly ( $P < 0.05$ ). The increasing treatment of EBE demonstrated a downregulation of *Bcl-xL* gene for  $EBE_{25}$ ,  $EBE_{50}$ , and  $EBE_{75}$  as compared to the untreated group, respectively. However, there was no significant difference observed between EBE treatments ( $P > 0.05$ ) on the regulation of *Bcl-xL* gene. In the meantime, cisplatin illustrated a dose-dependent upregulation of *Bcl-xL* gene compared to the untreated group, significantly ( $P < 0.05$ ). Protein profiles from both treatments resulted in a significant upregulation of Bcl-xL expression as compared to the untreated group ( $P < 0.05$ ). It was noted that the regulation of apoptotic mechanism in 2D and 3D WERI-Rb-1 models differed significantly upon treatment with EBE.

Subsequently, Figure 4 illustrated the gene and protein expressions of Caspase 3 and Caspase 9, respectively. *Caspase 3* gene was upregulated in a dose-dependent manner for all treatments compared to the untreated group, respectively. In the meantime, it was noted that only  $EBE_{25}$  and  $EBE_{50}$  treatments portrayed upregulation of Caspase 3 protein in comparison to other treatment groups, respectively ( $P < 0.05$ ). Besides that, the upregulation of *Caspase 9* gene was significantly increased in a concentration dependent manner for both treatments compared to the untreated group ( $P < 0.05$ ). A significant Caspase 9 upregulation was observed in  $EBE_{25}$  treatment against  $EBE_{50}$  and  $EBE_{75}$  ( $P < 0.05$ ) whereas, no significant different was detected between  $EBE_{50}$  and  $EBE_{75}$  treatments ( $P > 0.05$ ). Cisplatin demonstrated a significant modulation of Caspase 9 gene among treatments ( $P < 0.05$ ). Protein expression of Caspase 9 activity also revealed a significant upregulation against the untreated group, respectively ( $P < 0.05$ ). The effect of EBE was only observed between  $EBE_{25}$  and  $EBE_{75}$  ( $P < 0.05$ ) towards the upregulation of Caspase 9 protein. In addition, a remarkable treatment differences between EBE and cisplatin were noticed in Caspase 9 protein ( $P < 0.05$ ).

Figure 5A depicted a significant Nrf-2 upregulation upon EBE treatment as compared to cisplatin and untreated group ( $P < 0.05$ ), respectively. The EBE treatment also resulted in a higher Nrf-2 regulation compared to the cisplatin ( $P < 0.05$ ). Figure 5B displayed a significant fold-increase of Nrf-2 protein in cisplatin as compared to the EBE and untreated group

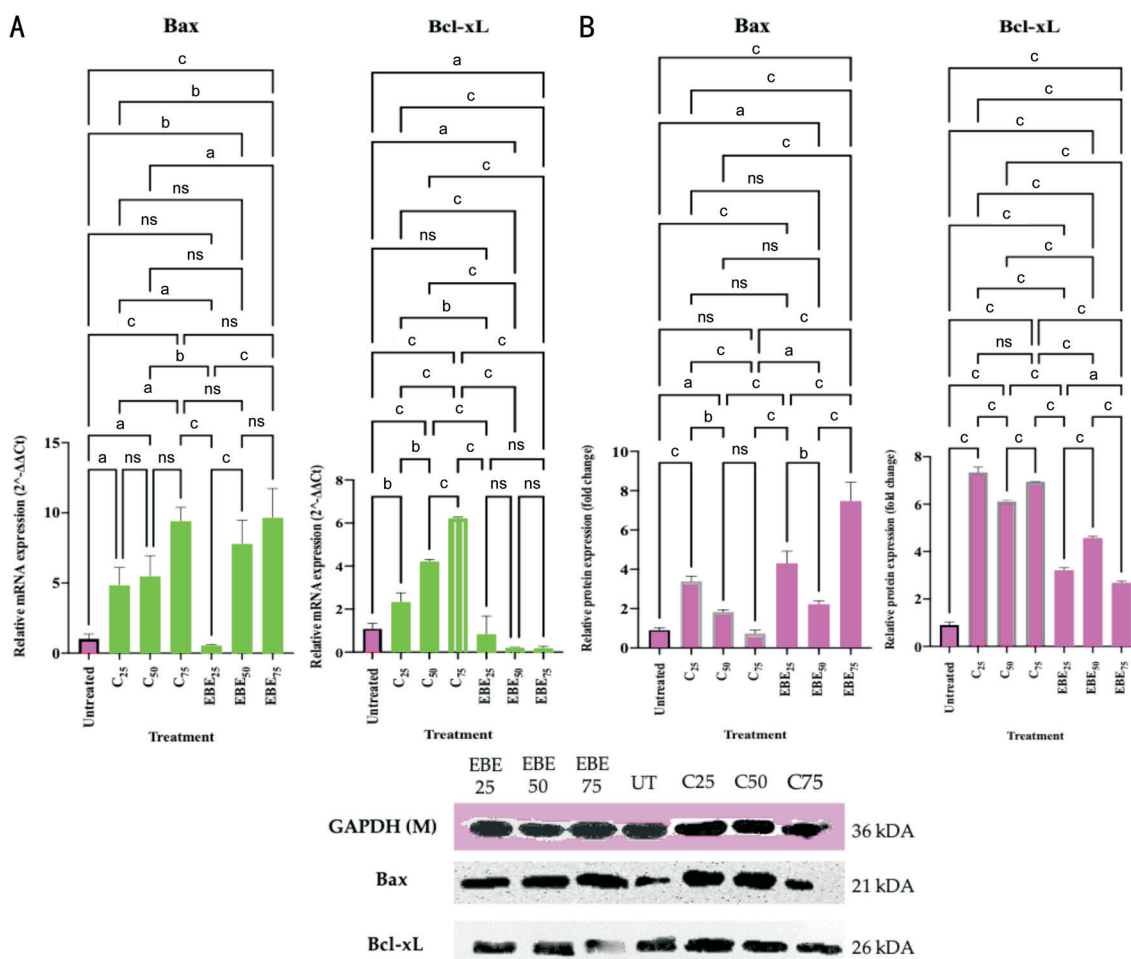


**Figure 3** Relative mRNA (A) and protein (B) expressions of Bax and Bcl-xL in 3D WERI-Rb-1 spheroids treated with EBE and cisplatin, respectively <sup>a</sup> $P < 0.05$ ; <sup>b</sup> $P < 0.01$ ; <sup>c</sup> $P < 0.001$ ; ns: Not significant. Bcl-xL: B-cell lymphoma-extra large; Bax: BCL-2 associated X; GAPDH: Glyceraldehyde-3-phosphate dehydrogenase; EBE: *Eleutherine bulbosa* (Mill.) Urb. bulb extract.

( $P < 0.05$ ), respectively. The EBE treatments recorded a slight upregulation of Nrf-2 protein compared to the untreated group ( $P < 0.05$ ) meanwhile, showing no significant difference within treatments ( $P > 0.05$ ), respectively. Besides that, the mRNA expression of *HO-1* gene revealed significance upregulation of EBE treatments as compared to the untreated group and cisplatin ( $P < 0.05$ ), respectively. Cisplatin showed a significant downregulation of *HO-1* gene in contrast to the untreated group ( $P < 0.05$ ), respectively. For protein profiles, the level of HO-1 protein was significantly downregulated upon receiving both treatments in 3D WERI-Rb-1 spheroids as compared to the untreated group ( $P < 0.05$ ). Furthermore, both treatments illustrated a significant decreasing trend on SOD-1 mRNA expression as compared to the untreated group, respectively. The immunoblot results revealed that SOD-1 protein was significantly upregulated in EBE compared to the untreated group ( $P < 0.05$ ), respectively.

**DISCUSSION**

Poor penetration of chemotherapeutic agents is one of the numerous factors affecting the  $IC_{50}$  value in 3D cell culture system. The presence of ECM regulates the natural tumor

microenvironment such as physiological gradient that may hinder direct drug penetration. ECM like Matrigel and collagen will regulate the adhesion proteins like E-cadherin and integrins by stimulating cell aggregates to form spheroid formation<sup>[18-20]</sup>. The resulting cell adhesions create a physical barrier that may dissolve and restrict drug penetration. Moreover, tissue architecture of a dense cellular morphology and density may also influence drug diffusion from blood vessels to cancer cells as well as into the spheroid structure<sup>[21-22]</sup>. On the contrary, cells cultured in a 2D monolayer is distributed evenly on a culture dish with direct exposure to the chemotherapeutic agents, leading to unreliable results<sup>[23]</sup>. A study carried out by Nowacka *et al*<sup>[23]</sup> demonstrated a remarkable cisplatin and paclitaxel resistance in 3D A2780 ovarian cancer. The drug resistant for cisplatin recorded a 10-fold increase meanwhile, paclitaxel recorded a 1098-fold increase in comparison between 2D and 3D cell cultures. Furthermore, the study performed by Koch *et al*<sup>[24]</sup> also revealed a significant increase of cisplatin ( $IC_{50}$ ) in a 3D spheroid model of HCT116 and SW480 colon cancer compared to 2D counterparts. Thus, our study revealed that the presence of the collagen restricts drug

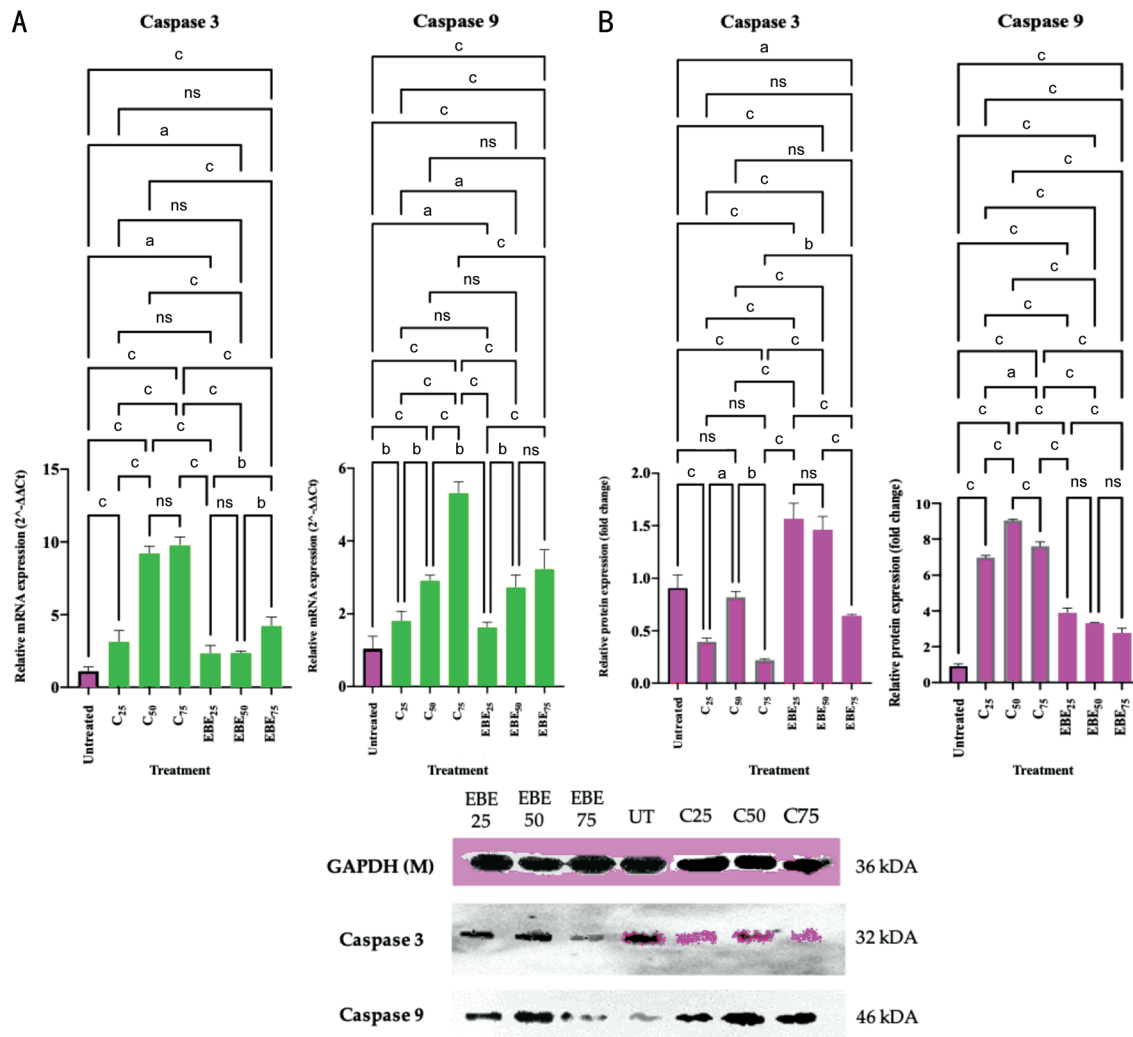


**Figure 4** Relative mRNA (A) and protein (B) expressions of Caspase 3 and Caspase 9 in 3D WERI-Rb-1 spheroids treated with EBE and cisplatin, respectively <sup>a</sup> $P < 0.05$ ; <sup>b</sup> $P < 0.01$ ; <sup>c</sup> $P < 0.001$ ; ns- not significant. Caspase: Cystein-aspartic acid protease; GAPDH: Glyceraldehyde-3-phosphate dehydrogenase; EBE: *Eleutherine bulbosa* (Mill.) Urb. bulb extract.

penetration, resulting in increased IC<sub>50</sub> values in the 3D WERI-Rb-1 spheroids. Moreover, both spheroids demonstrated cellular aggregation compared to their native 2D cultures. For WERI-Rb-1, the spheroids were aggregated (Group 3) similar to the work described<sup>[25]</sup>. The structural differences in both cultures could be associated with the dynamic variations in the 3D environment that promotes cellular activities such as cell proliferation, differentiation, migration, survivability, cell adhesion, cytoskeletal conformation, and cell signaling in natural tissue physiology. The intercalating red PI dye manifested apoptotic bodies such as membrane blebbing and chromatin condensation with increased concentrations in contrast to the untreated group. The untreated group representing viable cells demonstrated an intact membrane with less cellular damage fluoresced by the bright blue DAPI dye. The collagen fibers acting as an ECM matrix orchestrate the cytoskeletal organization of 3D spheroids by facilitating cellular signalling, cell movement, and nutrient diffusion. Besides that, cellular disruption and apoptotic bodies became

more apparent with increasing concentrations of EBE and cisplatin, respectively. The apoptotic effect of EBE could be associated with the synergistic interaction of the bioactive compounds reported in the previous study<sup>[6]</sup>. Little information is known on how drug-induced apoptotic mechanisms in WERI-Rb-1 cultured in a 3D environment. This part of the study documented the expression of various genes and proteins contributing to apoptosis. The effect between concentrations was also explored to further investigate the regulation of specific apoptosis-related genes and proteins. Overall, each gene and protein revealed a statistically significant difference in one-way ANOVA analysis ( $P < 0.05$ ). In our recent study, the Bcl-2 family members such as Bcl-2 and Bcl-xL were downregulated in 2D WERI-Rb-1 model, however, significantly upregulated in this study<sup>[5]</sup>. The variation between these models could be associated with the apoptotic resistance upon treatment due to the presence of ECM matrix that hinders drug penetration. According to Marquez *et al*<sup>[26]</sup>, the dysregulation of Bcl-2 family members

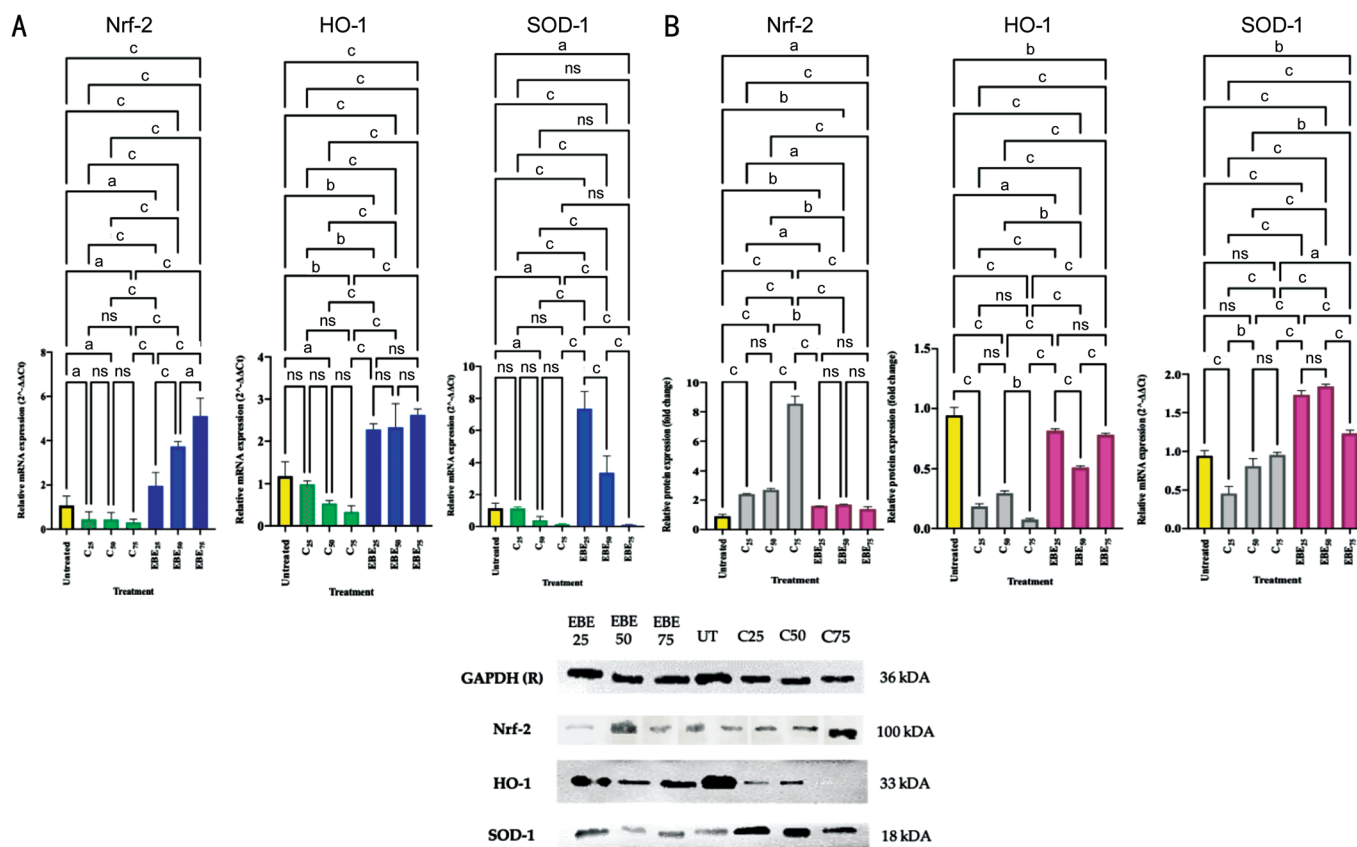


**Figure 5** The regulation of mRNA (A) and protein (B) expressions of Nrf-2, HO-1, and SOD-1 treated with EBE and cisplatin, respectively <sup>a</sup>*P*<0.05; <sup>b</sup>*P*<0.01; <sup>c</sup>*P*<0.001; ns: Not significant; EBE: *Eleutherine bulbosa* (Mill.) Urb. bulb extract; NRF-2: Nuclear factor erythroid 2-related factor; HO-1: Heme oxygenase 1; SOD-1: Superoxide dismutase 1; GAPDH: Glyceraldehyde-3-phosphate dehydrogenase.

such as overexpression of pro-survival genes and pro-apoptotic silencing are significant drivers for apoptotic resistance in cancer therapy. Thus, this could be explaining the relative increase of treatment concentrations in cytotoxic study between 3D and 2D WERI-Rb-1 cultures, as well as their genes and protein expressions.

Apoptosis is a genetically regulated and highly conserved mechanisms in multicellular organisms<sup>[27]</sup>. This homeostatic machinery primarily relies on the regulation of the caspase cascades to execute cell death, resulting in the proteolytic cleavage of numerous cytoskeletal and nuclear proteins<sup>[28]</sup>. Even though numerous additional types of cell death have been found and documented, the intrinsic apoptosis pathway remains physiologically dominant, killing about 60 billion of our cells every day<sup>[29-30]</sup>. The intrinsic pathway is primarily governed by the Bcl-2 family proteins that modulate the mitochondrial outer membrane permeabilization (MOMP). The resulting MOMP releases the apoptogenic proteins such as cytochrome c in the cytoplasmic membrane that would bind to the apoptotic protease-activating factor 1 (APAF-1). At this stage, there was no cellular point of return which triggers the initiator caspases like Caspase 9 and executioner caspases *i.e.*, Caspase 3 to dismantle cellular structures<sup>[29]</sup>. Thus, the results in this study indicated that the caspase cascades were activated,

causing apoptotic cell death.

The modulation of Nrf-2 pathway in numerous cancers promote the upregulation of the pro-survival genes and cell proliferation through metabolic reprogramming, apoptotic resistance, and self-renewal of cancer stem cells<sup>[31]</sup>. More importantly, the constitutive activation of Nrf-2 in cancer cells promote the apoptotic resistance. It could be proposed that the upregulation of Nrf-2 protein promotes the growth of retinoblastoma spheroids in ECM collagen matrix. The expression of Nrf-2 protein in WERI-Rb-1 treated spheroids were associated with the apoptotic escape, leading to tumor progression in the ECM environment. This might be associated with the cytoprotective properties of Nrf-2 protein that modulates the redox equilibrium and prevent cellular damage by reactive oxygen species (ROS)<sup>[31]</sup>. Thus, more cells escape the regulated machinery, resulting in tumor progression and treatment resistance. The event also confers the increased cytotoxic treatments necessary for apoptotic induction in 3D WERI-Rb-1 treated spheroids. Moreover, the upregulation of the Nrf-2 protein demonstrated a direct relationship with the Bcl-2 family expression. Studies reported by Nitire and Jaiswal<sup>[32]</sup> indicated that the upregulation of Nrf-2 protein-mediated the Bcl-2 expression, leading to the etoposide-induced apoptotic resistance and tumor progression.

Besides that, many cancers portray that the overexpression of collagen may result in proliferative oncogenic environment through structural and signaling interactions<sup>[33]</sup>. Trédan *et al*<sup>[34]</sup> proposed that the apoptotic sensitivity may be caused by numerous cytokines, hormones, growth factors, and extracellular matrix, leading to cell adhesion-mediated treatment resistance. As opposed to our findings in 2D WERI-Rb-1 culture, the regulation of the Nrf-2 protein could be clearly distinguished which confirmed that the different physiological conditions could affect treatment response<sup>[5]</sup>. Besides that, the mRNA expression of *HO-1* gene revealed significant upregulation of EBE treatments as compared to the untreated group and cisplatin ( $P<0.05$ ), respectively. Cisplatin showed a significant downregulation of *HO-1* gene in contrast to the untreated group ( $P<0.05$ ), respectively. For protein profiles, the level of HO-1 protein was significantly downregulated upon receiving both treatments in 3D WERI-Rb-1 spheroids as compared to the untreated group ( $P<0.05$ ). Furthermore, both treatments illustrated a significant decreasing trend in SOD-1 mRNA expression as compared to the untreated group. The immunoblot results revealed that SOD-1 protein was significantly upregulated in EBE compared to the untreated group ( $P<0.05$ ). The SOD-1 is well recognized for its involvement in redox homeostasis, and it is frequently dysregulated throughout cancer progression<sup>[35]</sup>. Li *et al*<sup>[35]</sup> documented that the knock-out of *SOD-1* gene demonstrated tumor inhibition in the nasopharyngeal carcinoma cells, *in vitro* and *in vivo*. The contradictory results of the SOD-1 in this study could be associated with treatment resistance due to the poor penetration of the extract under 3D environment. Due to the limited penetration and distribution, increasing ECM has been found to have a direct influence on the concentration of intratumor medication<sup>[36]</sup>.

In conclusion, it could be summarized that the WERI-Rb-1 spheroids in the ECM collagen matrix portrayed different morphological and molecular characteristics. The presence of ECM caused an increase in cytotoxic resistance upon treatment with EBE and cisplatin. The morphological assessment also revealed distinct morphological shapes and attributes between 2D and 3D models. The spheroids in ECM collagen matrix displayed cell-to-cell contact, resulting in cellular aggregation meanwhile in 2D model, WERI-Rb-1 cells lost their polarities, limiting their cellular growth. More importantly, EBE and cisplatin portrayed apoptotic features such as chromatin condensation, membrane blebbing, and apoptotic bodies. Both treatments displayed distinct upregulation and downregulation of apoptotic and antioxidant gene and protein expressions compared to our previous study on 2D WERI-Rb-1 cells. We proposed that the ECM collagen regulates the natural tumor microenvironment causing less drug penetration towards

the WERI-Rb-1 spheroids. It could be stated that the 3D WERI-Rb-1 spheroids was a reliable model for studying pharmacological mechanisms in contrast to a classic 2D model. We developed a low-cost method for 3D WERI-Rb-1 spheroids derived from the cell line using type I murine collagen. Future research should optimize the collagen concentration for optimum drug penetration and efficacies. Furthermore, in-depth studies such as animal experimentation is also warranted to observe the valuable insights of EBE as a chemotherapeutic compound for the treatment of retinoblastoma and other human malignancies.

#### ACKNOWLEDGEMENTS

**Foundation:** Supported by Universiti Putra Malaysia, Serdang, Selangor, Malaysia (UPM/700-2/1/GPB/2017/9549900).

**Authors' Contributions:** Conceived and designed the work (Kamarudin AA, Mohd Esa NM); Collected the data (Sayuti NH, Cheng ZHZ); Contributed data (Sayuti NH); Performed the analysis (Saad N); Wrote the paper (Kamarudin AA); Performed the analysis (Azmi NH); Final editing and approval (Saad N, Mohd Esa NM). All authors agree to be accountable for the content of the work.

**Conflicts of Interest:** Kamarudin AA, None; Sayuti NH, None; Cheng ZHZ, None; Saad N, None; Azmi NH, None; Mohd Esa N, None.

#### REFERENCES

- 1 Saengwimol D, Rojanaporn D, Chaitankar V, *et al*. A three-dimensional organoid model recapitulates tumorigenic aspects and drug responses of advanced human retinoblastoma. *Sci Rep* 2018;8(1):15664.
- 2 Ancona-Lezama D, Dalvin LA, Shields CL. Modern treatment of retinoblastoma: a 2020 review. *Indian J Ophthalmol* 2020;68(11):2356-2365.
- 3 Ieyama T, Gunawan-Puteri MD, Kawabata J.  $\alpha$ -Glucosidase inhibitors from the bulb of *Eleutherine Americana*. *Food Chem* 2011;128(2):308-311.
- 4 Kamarudin AA, Sayuti NH, Saad N, *et al*. *Eleutherine bulbosa* (mill.) urb. bulb: review of the pharmacological activities and its prospects for application. *Int J Mol Sci* 2021;22(13):6747.
- 5 Kamarudin AA, Sayuti NH, Saad N, *et al*. Induction of apoptosis by *Eleutherine bulbosa* (Mill.) Urb. bulb extracted under optimised extraction condition on human retinoblastoma cancer cells (WERI-Rb-1). *J Ethnopharmacol* 2022;284:114770.
- 6 Kamarudin AA, Esa NM, Saad N, *et al*. Heat assisted extraction of phenolic compounds from *Eleutherine bulbosa* (Mill.) bulb and its bioactive profiles using response surface methodology. *Ind Crops Prod* 2020;144:112064.
- 7 Biju TS, Priya VV, Francis AP. Role of three-dimensional cell culture in therapeutics and diagnostics: an updated review. *Drug Deliv Transl Res* 2023;13(9):2239-2253.
- 8 Langhans SA. Three-dimensional *in vitro* cell culture models in drug discovery and drug repositioning. *Front Pharmacol* 2018;9:6.
- 9 Abuwatfa WH, Pitt WG, Hussein GA. Scaffold-based 3D cell culture

- models in cancer research. *J Biomed Sci* 2024;31(1):7.
- 10 Karamanos NK, Theocharis AD, Piperigkou Z, *et al.* A guide to the composition and functions of the extracellular matrix. *FEBS J* 2021;288(24):6850-6912.
- 11 Ho TC, Chang CC, Chan HP, *et al.* Hydrogels: properties and applications in biomedicine. *Molecules* 2022;27(9):2902.
- 12 Feng B, Yang H, Zhu MM, *et al.* Collagen-based biomaterials in organoid technology for reproductive medicine: composition, characteristics, and applications. *Collagen Leather* 2023;5(1):35.
- 13 Solbu AA, Caballero D, Damigos S, *et al.* Assessing cell migration in hydrogels: an overview of relevant materials and methods. *Mater Today Bio* 2023;18:100537.
- 14 Rajan N, Habermehl J, Coté MF, *et al.* Preparation of ready-to-use, storable and reconstituted type I collagen from rat tail tendon for tissue engineering applications. *Nat Protoc* 2006;1(6):2753-2758.
- 15 Eilenberger C, Kratz SRA, Rothbauer M, *et al.* Optimized alamarBlue assay protocol for drug dose-response determination of 3D tumor spheroids. *MethodsX* 2018;5:781-787.
- 16 Roy AS, Tripathy DR, Samanta S, *et al.* DNA damaging, cell cytotoxicity and serum albumin binding efficacy of the rutin-Cu(ii) complex. *Mol Biosyst* 2016;12(5):1687-1701.
- 17 Toni LS, Garcia AM, Jeffrey DA, *et al.* Optimization of phenol-chloroform RNA extraction. *MethodsX* 2018;5:599-608.
- 18 Huang JC, Zhang LL, Wan DL, *et al.* Extracellular matrix and its therapeutic potential for cancer treatment. *Signal Transduct Target Ther* 2021;6(1):153.
- 19 Nicolas J, Magli S, Rabbachin L, *et al.* 3D extracellular matrix mimics: fundamental concepts and role of materials chemistry to influence stem cell fate. *Biomacromolecules* 2020;21(6):1968-1994.
- 20 Rodrigues DB, Reis RL, Pirraco RP. Modelling the complex nature of the tumor microenvironment: 3D tumor spheroids as an evolving tool. *J Biomed Sci* 2024;31(1):13.
- 21 Paajanen J, Laaksonen S, Kettunen E, *et al.* Histopathological features of epithelioid malignant pleural mesotheliomas in patients with extended survival. *Hum Pathol* 2020;98:110-119.
- 22 Roy SM, Garg V, Barman S, *et al.* Kinetics of nanomedicine in tumor spheroid as an *in vitro* model system for efficient tumor-targeted drug delivery with insights from mathematical models. *Front Bioeng Biotechnol* 2021;9:785937.
- 23 Nowacka M, Sterzynska K, Andrzejewska M, *et al.* Drug resistance evaluation in novel 3D *in vitro* model. *Biomedicine Pharmacother* 2021;138:111536.
- 24 Koch J, Mönch D, Maaß A, *et al.* Three dimensional cultivation increases chemo- and radioresistance of colorectal cancer cell lines. *PLoS One* 2021;16(1):e0244513.
- 25 Selby M, Delosh R, Laudeman J, *et al.* 3D models of the NCI60 cell lines for screening oncology compounds. *SLAS Discov* 2017;22(5):473-483.
- 26 Marquez RT, Tsao BW, Faust NF, *et al.* Apoptosis. *Drug resistance and molecular cancer therapy: Apoptosis versus autophagy*. UK: IntechOpen; 2013:155-177.
- 27 D'Arcy MS. Cell death: a review of the major forms of apoptosis, necrosis and autophagy. *Cell Biol Int* 2019;43(6):582-592.
- 28 Farghadani R, Naidu R. Resulation and dysfunction of apoptosis. *The role of apoptosis as a double-edge sword in cancer*. UK: IntechOpen; 2022:3-24.
- 29 Singh R, Letai A, Sarosiek K. Regulation of apoptosis in health and disease: the balancing act of BCL-2 family proteins. *Nat Rev Mol Cell Biol* 2019;20(3):175-193.
- 30 Bertheloot D, Latz E, Franklin BS. Necroptosis, pyroptosis and apoptosis: an intricate game of cell death. *Cell Mol Immunol* 2021;18(5):1106-1121.
- 31 Wu SJ, Lu H, Bai YH. Nrf2 in cancers: a double-edged sword. *Cancer Med* 2019;8(5):2252-2267.
- 32 Niture SK, Jaiswal AK. Nrf2 protein up-regulates antiapoptotic protein Bcl-2 and prevents cellular apoptosis. *J Biol Chem* 2012;287(13):9873-9886.
- 33 Khawar IA, Kim JH, Kuh HJ. Improving drug delivery to solid tumors: priming the tumor microenvironment. *J Control Release* 2015;201:78-89.
- 34 Trédan O, Galmarini CM, Patel K, *et al.* Drug resistance and the solid tumor microenvironment. *J Natl Cancer Inst* 2007;99(19):1441-1454.
- 35 Li S, Fu LY, Tian T, *et al.* Disrupting SOD1 activity inhibits cell growth and enhances lipid accumulation in nasopharyngeal carcinoma. *Cell Commun Signal* 2018;16(1):28.
- 36 Zargar A, Chang S, Kothari A, *et al.* Overcoming the challenges of cancer drug resistance through bacterial-mediated therapy. *Chronic Dis Transl Med* 2019;5(4):258-266.